X-763-70-353
PREPRINT

NASA TM X- 65354

TIME AND FUEL OPTIMAL CONTROL FOR GRAVITY GRADIENT SPACECRAFT

F. C. ZACH

SEPTEMBER 1970

GSFC

GODDARD SPACE FLIGHT CENTER
GREENBELT, MARYLAND

X-763-70-353

PREPRINT

TIME AND FUEL OPTIMAL CONTROL FOR GRAVITY GRADIENT SPACECRAFT

F. C. Zach

September 1970

GODDARD SPACE FLIGHT CENTER

Greenbelt, Maryland

PRECEDING PAGE BLANK NOT FILMED.

TIME AND FUEL OPTIMAL CONTROL FOR GRAVITY GRADIENT SPACECRAFT*

F. C. Zach

ABSTRACT

Severe constraints on the amount of fuel available in spacecraft make it necessary to develop economical policies for attitude control. A promising approach is to combine active control by means of electric propulsion devices and passive gravity gradient control. The Maximum Principle is used to derive a time-fuel optimal control law for gravity gradient satellites. Switching lines which make it possible to determine the optimal control for each measured set of angles and rates are derived for decoupled gravity gradient satellites. It is shown how by this technique the special cases of pure time optimal and pure fuel optimal control, which have been already solved in the literature, are covered. The possible extensions to coupled gravity gradient satellites are treated and it is shown that no unique switching lines can be derived.

*The work for this paper was accomplished while the author held a National Research Council Postdoctoral Resident Research Associateship supported by the National Aeronautics and Space Administration, Goddard Space Flight Center. The author is very much obliged to Mr. W. Isley and Mr. D. Endres for their valuable suggestions.

PRECEDING PAGE BLANK NOT FILMED.

CONTENTS

PRECEDING PAGE BLANK NOT FILMED.

NOMENCLATURE

The index i stands for yaw, roll and pitch and is omitted when no distinction in the treatment of the different axes is necessary.

a_j = gravity gradient coefficients, $j = x, y, z$

C_{mn} = centers of the switching circular arcs, $m = 1, 2, 3, 4$; $n = 1, 2, \cdots$

d_i = reduced disturbance torque ($= T_{di}/I_{ii}$), $i = x, y, z$

H = Hamiltonian

I_{ii} = moments of inertia, $i = x, y, z$

k = maximum absolute value of control u

P = performance index

p_m = auxiliary variables, $m = 0, 1, \cdots n$

T_{ci} = control torque, $i = x, y, z$

T_{di} = disturbance torque, $i = x, y, z$

t = time

t_c = time interval where control is on

t_e = time of control end

t_{off} = time interval where control is off

t_o = time of control start

u_i = reduced control torque ($= T_{ci}/I_{ii}$), $i = x, y, z$

x = state variable

x_{mn}, y_{mn} = cartesian coordinates of the centers of the switching circular arcs, $m = 1, 2, 3, 4$; $n = 1, 2, \cdots$

y_{cm} = y-coordinates of the switching circular arcs, m = 1, 2, 3, 4

α = pitch angle (corresponds to z-axis)

β = maximum angle of circular arcs in thrusting periods

Γ_+ = line for switching from u = 0 to u = +k

Γ_- = line for switching from u = 0 to u = - k

γ = maximum angle of circular arcs in coasting periods

Λ_+ = line for switching from u = k to u = 0

Λ_- = line for switching from u = - k to u = 0

λ_f = weighting factor for fuel in the performance index P

λ_t = weighting factor for time in the performance index P

ρ_{mn}, φ_{mn} = polar coordinates of the centers of the switching arcs, m = 1, 2, 3, 4; n = 1, 2, · · ·

ϕ = roll angle (corresponds to y-axis)

ψ = yaw angle (corresponds to x-axis)

ω_0 = orbital angular rate for circular equatorial orbit

TIME AND FUEL OPTIMAL CONTROL FOR GRAVITY GRADIENT SPACECRAFT

INTRODUCTION

Attitude control of spacecraft requires economic use of fuel in order to maximize the number of control maneuvers for a specified amount of fuel. A promising approach is to combine active control by means of electric propulsion devices[1,2] and passive gravity gradient (GG) control. It has been shown in Reference 2 that the Maximum Principle can be used to derive the exact time optimal control law for gravity gradient satellites (GGS) if there is no coupling between the axes. However, if fuel constraints have to be imposed, consideration of fuel consumption in the optimum control law is necessary. An approximate solution has been derived in Reference 3 for GGSs with decoupled axes and in Reference 4 for general GGSs. The approximations made in these references make it necessary to shift the switching lines in the phase plane according to the initial angles and rates.

In the work performed here the exact solution for time/fuel optimal control of decoupled GGSs will be derived first. It will then be shown how the special cases of pure time optimal control as derived in References 2, 5, 6 and 7 and pure fuel optimal control (Reference 3) result from this approach.

The possible extension of this time-fuel optimal control law to coupled GGSs will be given.

Control maneuvers treated here bring initial angles and rates which can be caused by disturbances to zero. Pointing in other directions can be treated as in Reference 2.

TIME-FUEL OPTIMAL CONTROL FOR GGSs WITH UNCOUPLED AXES

It has been shown in References 2 and 8 that the small angle equations of motion for a gravity gradient satellite in a nearly circular equatorial orbit with negligible inner damping can be written as

$$I_{xx}\ddot{\psi} + \omega_0^2\left(I_{zz} - I_{yy}\right)\psi + \left(I_{zz} - I_{yy} - I_{xx}\right)\omega_0\dot{\phi} = T_{cx} + T_{dx} \tag{1}$$

$$I_{yy}\ddot{\phi} + 4\omega_0^2\left(I_{zz} - I_{xx}\right)\phi + \left(I_{xx} + I_{yy} - I_{zz}\right)\omega_0\dot{\psi} = T_{cy} + T_{dy} \tag{2}$$

$$I_{zz}\ddot{\alpha} + 3\omega_0^2\left(I_{yy} - I_{xx}\right)\alpha = T_{cz} + T_{dz} \tag{3}$$

If it is assumed that

$$I_{zz} = I_{xx} + I_{yy} \tag{4}$$

the cross-coupling between the yaw and roll axes is eliminated. In this case the equations of motion can be written as:

$$\ddot{\psi} + a_\psi \psi = u_\psi + d_\psi, \qquad \ddot{\phi} + a_\phi \phi = u_\phi + d_\phi \tag{5}$$

and

$$\ddot{\alpha} + a_\alpha \alpha = u_\alpha + d_\alpha, \tag{6}$$

where

$$a_\psi = \omega_0^2 \left(I_{zz} - I_{yy}\right)/I_{xx} , \qquad a_\phi = 4\omega_0^2 \left(I_{zz} - I_{xx}\right)/I_{yy} \tag{7}$$

$$a_\alpha = 3\omega_0^2 \left(I_{yy} - I_{xx}\right)/I_{zz} \tag{8}$$

$$u_\psi = T_{cx}/I_{xx} , \qquad u_\phi = T_{cy}/I_{yy} , \qquad u_\alpha = T_{cz}/I_{zz} \tag{9}$$

$$d_\psi = T_{dx}/I_{xx} , \qquad d_\phi = T_{dy}/I_{yy} , \qquad d_\alpha = T_{dz}/I_{zz} \tag{10}$$

It is assumed that the u_i are constrained in magnitude, i.e.

$$-k_i \leq u_i \leq k_i \qquad \text{for} \quad i = \alpha, \phi, \psi \tag{11}$$

If a disturbance free case ($d_\psi = d_\phi = d_\alpha = 0$) and constant control ($u_\psi$, u_ϕ, u_α = constant) is considered, circles for the phase plots are obtained in the (ψ, $\dot\psi a_\psi^{-1/2}$), (ϕ, $\dot\phi a_\phi^{-1/2}$) and (α, $\dot\alpha a_\alpha^{-1/2}$) phase planes,[2] providing that a_ψ, a_ϕ and $a_\alpha \neq 0$. The centers of these circles are at $\pm k_i/a_i$ with $i = \psi, \phi, \alpha$. For a_ψ, a_ϕ or $a_\alpha = 0$ parabolas are obtained. For this case the solution for time-fuel optimal control has been derived in Reference 1.

Equations (5) and (6) can be written as

$$\ddot{x} + ax = u \tag{12}$$

where $x = \psi, \phi, \alpha$, $a = a_\psi, a_\phi, a_\alpha$, $u = u_\psi, u_\phi, u_\alpha$ and $-k \leq u \leq +k$.

The Maximum Principle[5-7] will be applied to derive the time-fuel optimal control for Equation (12) in order to drive x and $\dot{x}$ to zero. The following procedure has to be applied:

(a) the performance index P has to be defined; for time-fuel optimal control

$$P = \int_{t_o}^{t_e} \left(\lambda_t + \lambda_f \, |u|\right) dt \tag{13}$$

where t_o is the start and t_e the end of control action. λ_t is the time weighting factor, λ_f the fuel weighting factor. E.g. $\lambda_f = 0$ leads to a pure time optimal solution.

(b) the mathematical model of the system has to be written in the form of first order linear differential equations

$$\dot{x}_i = f_i(\mathbf{x}, \mathbf{u}) \qquad (i = 0, 1, \cdots n) \tag{14}$$

n is the order of the system equations, $\mathbf{x}$ is the vector of the state variables $(x_0 \cdots x_n)$ and $\mathbf{u}$ is the vector of the control variables $(u_0 \cdots u_n)$.

(c) the Hamiltonian

$$H = \sum_{i=0}^{n} p_i \, f_i(\mathbf{x}, \mathbf{u}) \tag{15}$$

has to be maximized where $p_0 \cdots p_n$ are auxiliary variables given by

$$dp_i/dt = -\,\partial H/\partial x_i \quad \text{and} \quad dx_i/dt = \partial H/\partial p_i \qquad (i = 0, 1, \cdots n) \tag{16}$$

It is shown in References 5—7 that for this case $p_0 = -1$ can be chosen and that

$$\dot{x}_0 = f_0(\mathbf{x}, \mathbf{u}) = \lambda_t + \lambda_f |u| \tag{17}$$

In the case treated here

$$\mathbf{x} = \begin{bmatrix} x_0 \\ x_1 \\ x_2 \end{bmatrix} \qquad \dot{\mathbf{x}} = \begin{bmatrix} \dot{x}_0 \\ \dot{x}_1 \\ \dot{x}_2 \end{bmatrix} \tag{18}$$

which leads to

$$H = p_1 x_2 + p_2 (u - ax_1) - \lambda_t - \lambda_f |u| \tag{19}$$

H is maximized at every instant of time by

$$u = k \operatorname{sgn} p_2 \quad \text{for} \quad |p_2| \geq \lambda_f \tag{20}$$

and

$$u = 0 \quad \text{for} \quad |p_2| < \lambda_f \tag{21}$$

With Equations (16) and (19) one obtains

$$p_2 = P_m \sin\left(a^{1/2} t + \varphi\right) \tag{22}$$

where P_m and φ are integration constants.

The final arc: Figure 1 shows p_2 and u versus time t. From this figure it can be seen that u has to be on and off periodically. Furthermore, it can be said that u has to be on at the final time t_e; this is true since the state would never reach the origin with control off because in this case the trajectories are circles with the origin as center. The on time before reaching the origin is between 0 and t_c, t_c being the maximum on time. Therefore the part of the trajectory which leads the state to the origin has to be part of a semicircle with its center at $+k/a$ or $-k/a$ as shown in Figure 2. The longest arc leading to the origin is given by $\beta = \omega t_c$.

Coasting before final arc: From Figure 1 it is obvious that the state has to have a coasting period before reaching this final arc unless the initial condition happened to be on this final arc. The length of the coasting period is limited by $\gamma = \omega t_{off}$. If the initial conditions are far enough from the origin that more thrust intervals than the final one leading to the origin are required to drive the state to the origin the coasting interval is given by $\gamma = \omega t_{off}$. This means that by going back in time by t_{off} the time of switching from control to coasting has been found. In the phase plane this can be depicted by drawing circular arcs with the center in the origin and starting at each point of the arcs of Figure 2. The length of these arcs for coasting is given by γ. The endpoints of these arcs again form circle arcs which are produced by rotating the circle arcs of Figure 2 by an angle counter clockwise about the origin. This is shown in Figure 3. It can be seen from this figure that each initial state lying within the hatched area can be brought to the origin in a time-fuel optimal maneuver by coasting to Γ_+ or Γ_-, respectively and then by control application.

Thrusting before final coasting period: If the initial state does not lie in the hatched area of Figure 3 one sees from Figures 1 and 3 that another thrusting period is required with control of the reverse sign when compared with the final control. This thrusting period again can last up to a time interval t_c. Again shorter intervals than t_c for thrustings are applicable for cases where the initial condition is located such that it can be brought to Λ_- by thrusting intervals less than t_c. In the general case of thrust application of exactly t_c duration all possible trajectories for this period again are circular arcs with an angle β and their centers at $-k/a$ or $+k/a$, respectively. This means that the geometric locus of their starting points can be constructed by rotation of Λ_- or Λ_+, respectively, in Figure 3 counterclockwise by an angle β. The result is shown in Figure 4.

Complete switching lines: The procedures outlined can be pursued in the same manner as above. The geometric relationship produced by rotating the circle arcs by β or γ, respectively, show that all arcs which form the switching lines have their center on straight lines as shown in Figure 5. Also, the intersection points of the arcs lie on a straight line.

With $y = xa^{-1/2}$ the centers C_{1n} of the circular arcs for $n = 1, 2, \cdots$ are given by

$$x_{1n} = \rho_{1n} \cos \varphi_{1n} , \qquad y_{1n} = \rho_{1n} \sin \varphi_{1n} \tag{23}$$

where

$$\rho_{1n} = R\left\{\left[n(1 + \cos\gamma) - 1\right]^2 + [n \sin\gamma]^2\right\}^{1/2} \tag{24}$$

$$\varphi_{1n} = \arctan\left\{n \sin\gamma/\left[n(1 + \cos\gamma) - 1\right]\right\} \tag{25}$$

$$R = k/a \tag{26}$$

The equations of the circular arcs are then

$$y_{c1} = y_{1n} - \left[R^2 - \left(x - x_{1n}\right)\right]^{1/2} \tag{27}$$

$$\text{for} \quad (n-1)\,R(1 + \cos\gamma) \leq x \leq nR(1 + \cos\gamma) \tag{28}$$

To find the n corresponding to a given x the following equation can be applied

$$n = \text{Integer}\left[x/R(1 + \cos\gamma)\right] + 1 \qquad (x \geq 0) \tag{29}$$

The equations for the centers C_{2n} in the upper left hand quadrant are:

$$x_{2n} = -\rho_{2n} \cos\varphi_{2n}, \qquad y_{2n} = -\rho_{2n} \sin\varphi_{2n} \tag{30}$$

$$\rho_{2n} = R\left\{\left[n(1 + \cos\gamma) - \cos\gamma\right]^2 + \left[(n-1)\sin\gamma\right]^2\right\}^{1/2} \tag{31}$$

$$\varphi_{2n} = -\arctan\left\{(n-1)\sin\gamma/\left[n(1 + \cos\gamma) - \cos\gamma\right]\right\} \tag{32}$$

$$y_{c2} = y_{2n} + \left[R^2 - \left(x - x_{2n}\right)^2\right]^{1/2} \tag{33}$$

for

$$-nR(1+\cos\gamma) \leq x \leq -(n-1)\,R(1+\cos\gamma) \tag{34}$$

n for a given x can be found by

$$n = \text{Integer}\left[-x/R(1+\cos\gamma)+1\right] \qquad (x \leq 0) \tag{35}$$

The equations for the centers C_{3n} in the lower left hand quadrant are:

$$x_{3n} = -\rho_{3n}\cos\varphi_{3n}, \qquad y_{3n} = -\rho_{3n}\sin\varphi_{3n} \tag{36}$$

$$\rho_{3n} = \rho_{1n}, \qquad \varphi_{3n} = \varphi_{1n} \tag{37}$$

$$y_{c3} = y_{3n} + \left[R^2 - \left(x - x_{3n}\right)^2\right]^{1/2} \tag{38}$$

for

$$-nR(1+\cos\gamma) \leq x \leq -(n-1)\,R(1+\cos\gamma) \tag{39}$$

n for a certain x is given by Equation (35).

For the centers C_{4n} in the lower right hand quadrant the following equations hold

$$x_{4n} = \rho_{4n}\cos\varphi_{4n}, \qquad y_{4n} = \rho_{4n}\sin\varphi_{4n} \tag{40}$$

$$\rho_{4n} = \rho_{2n}, \qquad \varphi_{4n} = \varphi_{2n} \tag{41}$$

$$y_{c4} = y_{4n} - \left[R^2 - \left(x - x_{4n}\right)^2\right]^{1/2} \tag{42}$$

for x given by inequality (28).

n for a certain x is given by Equation (29).

Based upon Equations (23—42) the time/fuel optimal control law can be given by the flow chart of Figure 6.

REDUCTION OF THE GENERAL TIME-FUEL OPTIMAL CONTROL TO PURE TIME AND PURE FUEL OPTIMAL CONTROL

For the case where $\lambda_f = 0$ the pure time optimal control law is derived. This means for the switching lines that $\gamma = 0$ which leads to the well known semicircles as switching lines for the system with Equation (12). (Figure 7 and References 2, 5—7).

On the other hand, for $\lambda_t = 0$ the pure fuel optimal control law is derived. In this case thrusting is only provided when the state is exactly on the $\dot{x}a^{-1/2}$-axis, which means an impulse at this time. This corresponds with the results derived in Reference 3, where it is shown that most economic control for a system given by Equation 12 is achieved when the thruster is only in operation when the state falls on the $\dot{x}a^{-1/2}$- axis.

OPTIMAL CONTROL OF GRAVITY GRADIENT SATELLITES WITH COUPLED AXES

In the case where one principal moment of inertia is not equal to the sum of the two others the full GGS Equations (1)—(3) have to be considered. With

Equations (7)—(9) these can be written in the form:

$$\ddot{\psi} + a_\psi \psi - \left(1 - a_\psi/\omega_0^2\right) \omega_0 \dot{\phi} = u_\psi + d_\psi \tag{43}$$

$$\ddot{\phi} + a_\phi \phi + \left(1 - a_\phi/4\omega_0^2\right) \omega_0 \dot{\psi} = u_\phi + d_\phi \tag{44}$$

and

$$\ddot{\alpha} + a_\alpha \alpha = u_\alpha + d_\alpha \tag{45}$$

For the pitch equation the optimal control law derived above is still applicable; however, roll and yaw are now coupled. In order to calculate an optimal control law the following transformations have to be made to make application of Equations (15) and (16) possible:

$$a_1 = a_\psi/\omega_0^2 , \qquad a_2 = a_\phi/\omega_0^2 \tag{46}$$

The time base shall be changed to $\tau = \omega_0 t$. Therefore

$$d/dt = \omega_0\, d/d\tau \quad \text{or} \quad \dot{\psi} = \omega_0 \dot{\psi} \quad \text{and} \quad \dot{\phi} = \omega_0 \dot{\phi} \tag{47}$$

which gives for Equations (43—44)

$$\ddot{\psi} + a_1 \psi + b_1 \dot{\phi} = \bar{u}_\psi \tag{48}$$

and

$$\ddot{\phi} + a_2 \phi + b_2 \dot{\psi} = \bar{u}_\phi \tag{49}$$

with

$$\bar{u}_i = u_i/\omega_0^2 \qquad (i = \psi, \phi) \tag{50}$$

and

$$b_1 = a_1 - 1 , \qquad b_2 = 1 - a_2/4 \tag{51}$$

The following substitutions are made:

$$\psi = x_1 , \qquad \dot{\psi} = x_2 , \qquad \phi = x_3 , \qquad \dot{\phi} = x_4 \tag{52}$$

This yields for Equations (48—49):

$$\begin{aligned} \dot{x}_1 &= x_2 \\ \dot{x}_2 &= - a_1 x_1 - b_1 x_4 + \bar{u}_\psi \end{aligned} \tag{53}$$

$$\begin{aligned} \dot{x}_3 &= x_4 \\ \dot{x}_4 &= - a_2 x_3 - b_2 x_2 + \bar{u}_\phi \end{aligned} \tag{54}$$

The performance index for time-fuel optimal control is

$$P = \int_{t_0}^{t_e} \left[\lambda_t + \lambda_f \left(|\bar{u}_\psi| + |\bar{u}_\phi|\right)\right] dt \tag{55}$$

which gives

$$\dot{x}_0 = \lambda_t + \lambda_f \left(|\bar{u}_\psi| + |\bar{u}_\phi|\right) \tag{56}$$

The Hamiltonian is:

$$H = -\lambda_t - \lambda_f \left(|\bar{u}_\psi| + |\bar{u}_\phi| \right) + p_1 x_2 + p_2 \left(-a_1 x_1 - b_1 x_4 \right)$$

$$+ p_2 \bar{u}_\psi + p_3 x_4 + p_4 \left(-a_2 x_3 - b_2 x_2 \right) + p_4 \bar{u}_\phi \qquad (57)$$

which is maximized by:

$$\bar{u}_\psi = k_\psi \operatorname{sgn} p_2 \quad \text{for} \quad |p_2| \geq \lambda_f \qquad (58)$$

$$\bar{u}_\psi = 0 \quad \text{for} \quad |p_2| < \lambda_f \qquad (59)$$

$$\bar{u}_\phi = k_\phi \operatorname{sgn} p_4 \quad \text{for} \quad |p_4| \geq \lambda_f \qquad (60)$$

$$\bar{u}_\phi = 0 \quad \text{for} \quad |p_2| < \lambda_f \qquad (61)$$

Applying Equation (16) to Equation (37) yields:

$$\dot{p}_1 = a_1 p_2, \quad \dot{p}_2 = -p_1 + b_2 p_4, \quad \dot{p}_3 = a_2 p_4, \quad \dot{p}_4 = -p_3 + b_1 p_2 \qquad (62)$$

and

$$\ddddot{p}_2 + A_1 \ddot{p}_2 + A_2 = 0 \qquad (63)$$

$$\ddddot{p}_4 + A_1 \ddot{p}_4 + A_2 = 0 \qquad (64)$$

with

$$A_1 = a_1 + a_2 - b_1 b_2 \quad \text{and} \quad A_2 = a_1 a_2 \tag{65}$$

The roll and yaw equations can be written in a similar form if $\bar{u}_\phi$ and $\bar{u}_\psi$ are constant:

$$\ddddot{\phi} + A_1 \ddot{\phi} + A_2 = a_1 \bar{u}_\phi \tag{66}$$

$$\ddddot{\psi} + A_1 \ddot{\psi} + A_2 = a_2 \bar{u}_\psi \tag{67}$$

The solutions for Equations (63) and (64) are:

$$p_2 = P_{21} \sin\left(\tau + \varphi_1\right) + P_{22} \sin\left(A_2^{1/2} \tau + \varphi_2\right) \tag{68}$$

$$p_4 = -\left(b_1/b_2\right) P_{21} \cos\left(\tau + \varphi_1\right) - \left(a_1/a_2\right)^{1/2} P_{22} \cos\left(A_2^{1/2} \tau + \varphi_2\right) \tag{69}$$

For evaluation of the inequalities (58)—(61) only P_{21}/P_{22} (instead of P_{21} and P_{22} separately) is interesting since λ_f also is only interesting as its ratio to λ_t for the performance index. To find trajectories similar to the case with decoupled axes a transformation is made for Equations (66) and (67) by

$$x_1 = \ddot{\phi} + \phi \, , \qquad x_3 = \ddot{\psi} + \psi \tag{70}$$

which results in

$$\ddot{x}_1 + A_2 x_1 = a_1 \bar{u}_\phi \, , \qquad \ddot{x}_3 + A_2 x_3 = a_2 \bar{u}_\psi \tag{71}$$

Furthermore letting

$$\dot{x}_1 = x_2 , \qquad \dot{x}_3 = x_4$$

Equations (71) give circles in the (x_1, x_2) and (x_3, x_4) phase planes for $\bar{u}_\phi$ and $\bar{u}_\psi$ constant.

To find the switching lines in these phase planes in analogy to the decoupled case, variation of φ_1, φ_2 and P_{21}/P_{22} in Equations (68) and (69) and fullfillment of the inequalities (58)—(61) as function of time in connection with the system time history in the (x_1, x_2) and (x_3, x_4) phase planes is required.

However, no unique solution can be found. This is explained as follows:

For the decoupled case the solution of the adjoint equation for roll and yaw is determined only by a phase angle φ (see Equation 22) which corresponds with the phase angles φ_1 and φ_2 in Equations (68)—(69). Due to coupling effects also P_{21}/P_{22} has to be given in order to evaluate inequalities (58)—(61). But P_{21}/P_{22} not only depends on the coefficients b_1 and b_2 which determine the amount of crosscoupling but also on the initial conditions. The latter statement can easily be understood by the fact, that the switching sequence for one axis has to be much different whether the initial conditions on the other axis are large or small. This can be seen especially in these cases where the initial conditions are zero on one axis and $\neq 0$ on the other axis. In the decoupled case no control is required on the axis with initial conditions $= 0$. However, in the coupled case considerable control action may be necessary also on the axis with zero initial conditions.

This fact has been the subject of experimental investigations on an analog computer and the optimum switching sequence for special cases has been found by trial and error methods.[4]

CONCLUSIONS

Time-fuel optimal control procedures have been derived for gravity gradient satellites where yaw and roll axes are decoupled. It has been shown that for the coupled case no switching lines can be found. (Switching lines are necessary for the practical application of an optimal control law because the control strategy has to be based on the state of the system.) Therefore, it is recommended to try to decouple the yaw and roll axes of gravity gradient satellites by proper choice of moments of inertia if optimal control laws are to be applied. As one sees from the flow chart the control law is easy to apply. Choice of one parameter in the performance index covers the whole range between pure time and pure fuel optimal control.

REFERENCES

1. Isley, W. C., "Optimal Control Application for Electrothermal Multijet Systems on Synchronous Earth Spacecraft," Journal of Spacecraft and Rockets, Vol. 5, No. 12, Dec. 1968, pp. 1444-1451.

2. Zach, F. C., "Time Optimal Control of Gravity Gradient Satellites with Disturbances," X-734-69-501, NASA Goddard Space Flight Center, Nov. 1969, to be printed in Journal of Spacecraft and Rockets.

3. Flügge-Lotz, I., Craig, A. J., "The Choice of Time for Zeroing a Disturbance in a Minimum-Fuel Consumption Control Problem," Trans. ASME, Journal of Basic Engineering, March 1965, pp. 29-38.

4. Flügge-Lotz, I., Craig, A. J., "Investigation of Optimum Control With a Minimum-Fuel Consumption Criterion for a Fourth-Order Plant With Two Control Inputs; Synthesis of an Efficient Suboptimal Control." Trans. ASME, Journal of Basic Engineering, March 1965, pp. 39-57.

5. Pontryagin, L. S. et al., "The Mathematical Theory of Optimal Processes," Pergamon Press, Oxford, England 1964.

6. Athans, M., Falb, P. L., "Optimal Control," McGraw-Hill, New York 1966.

7. McCausland, I., "Introduction to Optimal Control," Wiley, New York 1969.

8. Frick, R. H., "Perturbation of a Gravity Gradient Stabilization System," Report AD 623279, The Rand Corporation, Santa Monica, Calif., Sept. 1965.

9. Barrett, C. C., "The Development of a Mathematical Model and a Study of One Method of Orbit Adjust and Station Keeping Gravity-Oriented Satellites," TN D-3652, Nov. 1966, NASA.

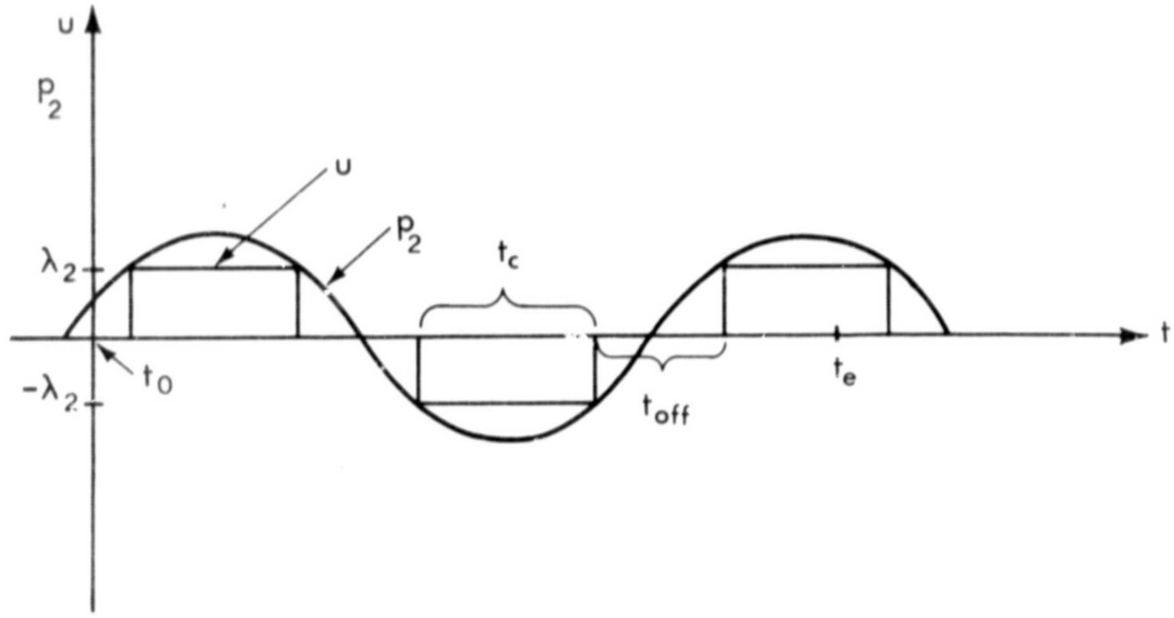

Figure 1. Control u and auxiliary variable p_2 for time-fuel optimal control of the plant

$\ddot{x} + ax = u$.

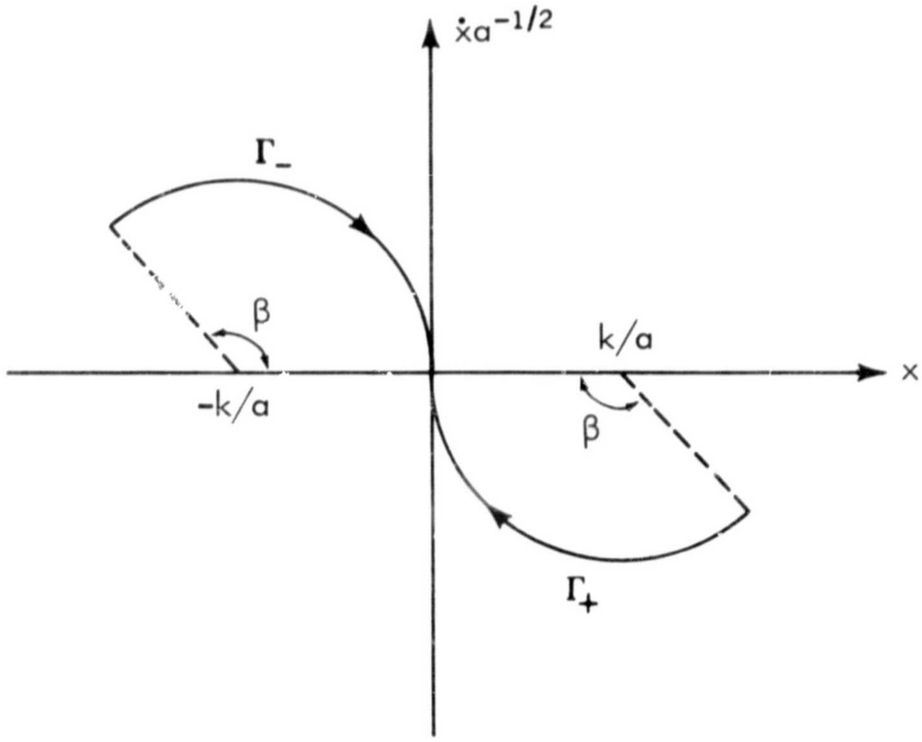

Figure 2. Final Arc: This last part of the optim... trajectory leads to the origin. The maximum duration of this arc is given by $\beta = \omega t_c$.

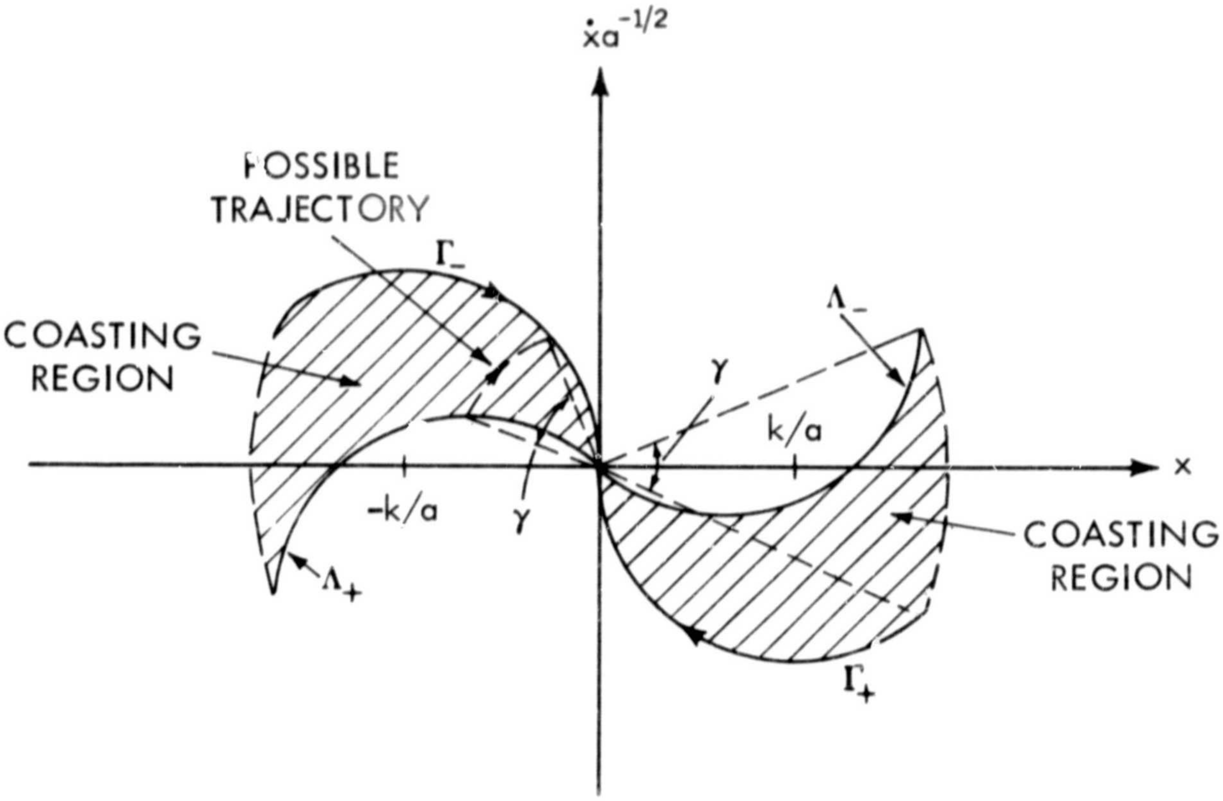

Figure 3. Coasting regions and switching lines. Between positive and negative thrust periods coasting periods are present whose length is given by γ.

Γ_+ ··· line for switching from $u = 0$ to $+k$

Γ_- ··· line for switching from $u = 0$ to $-k$

Λ_+ ··· line for switching from $u = +k$ to 0

Λ_- ··· line for switching from $u = -k$ to 0

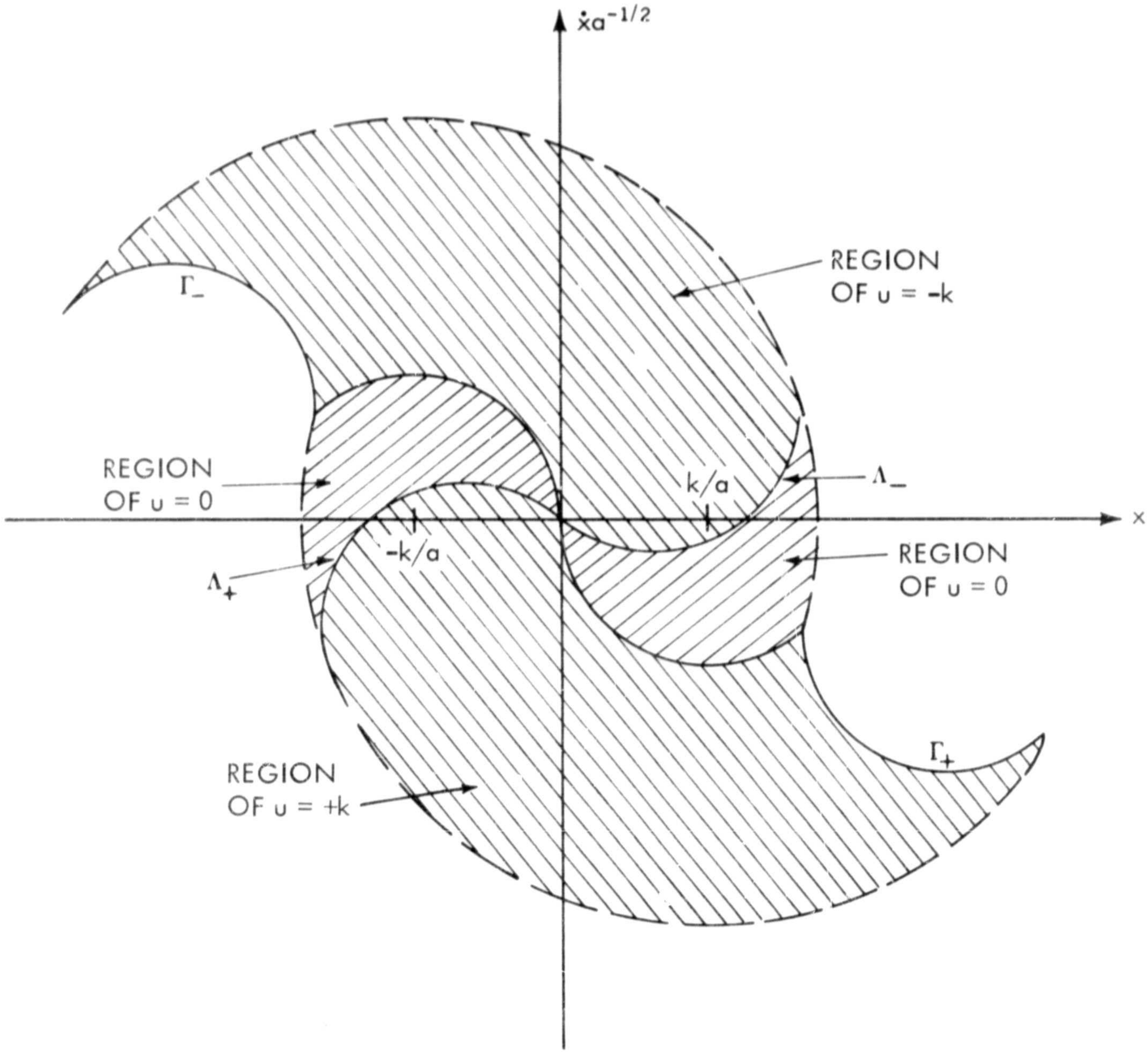

Figure 4. Extension of Figure 3 to show regions where thrust is applied before the state reaches the coasting regions shown in Figure 3.

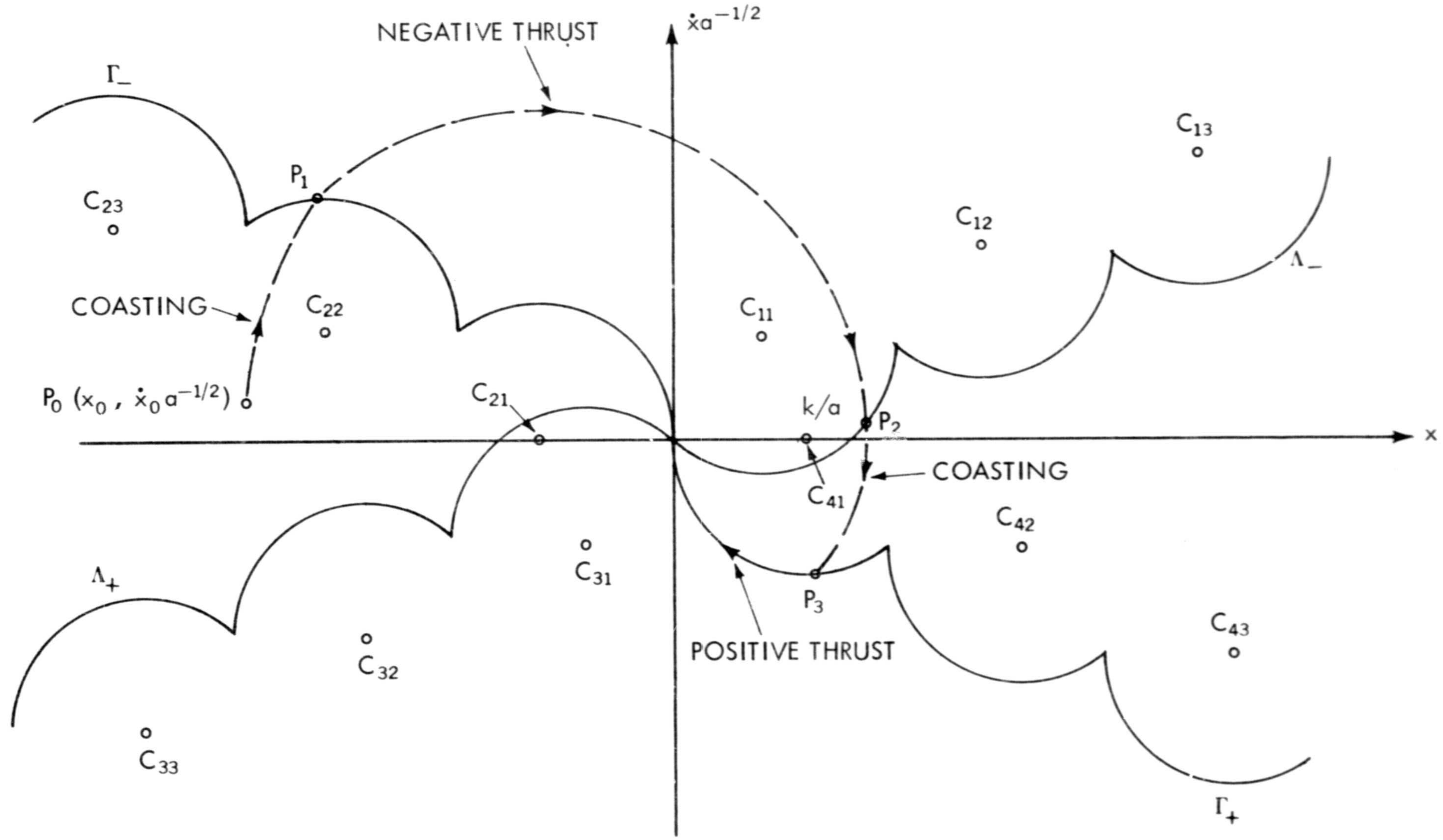

Figure 5. Switching lines for time-fuel optimal control with an example for an optimal trajectory, starting at P_0 and with switching at P_1, P_2, and P_3; C_{ik} ··· centers of switching circle arcs.

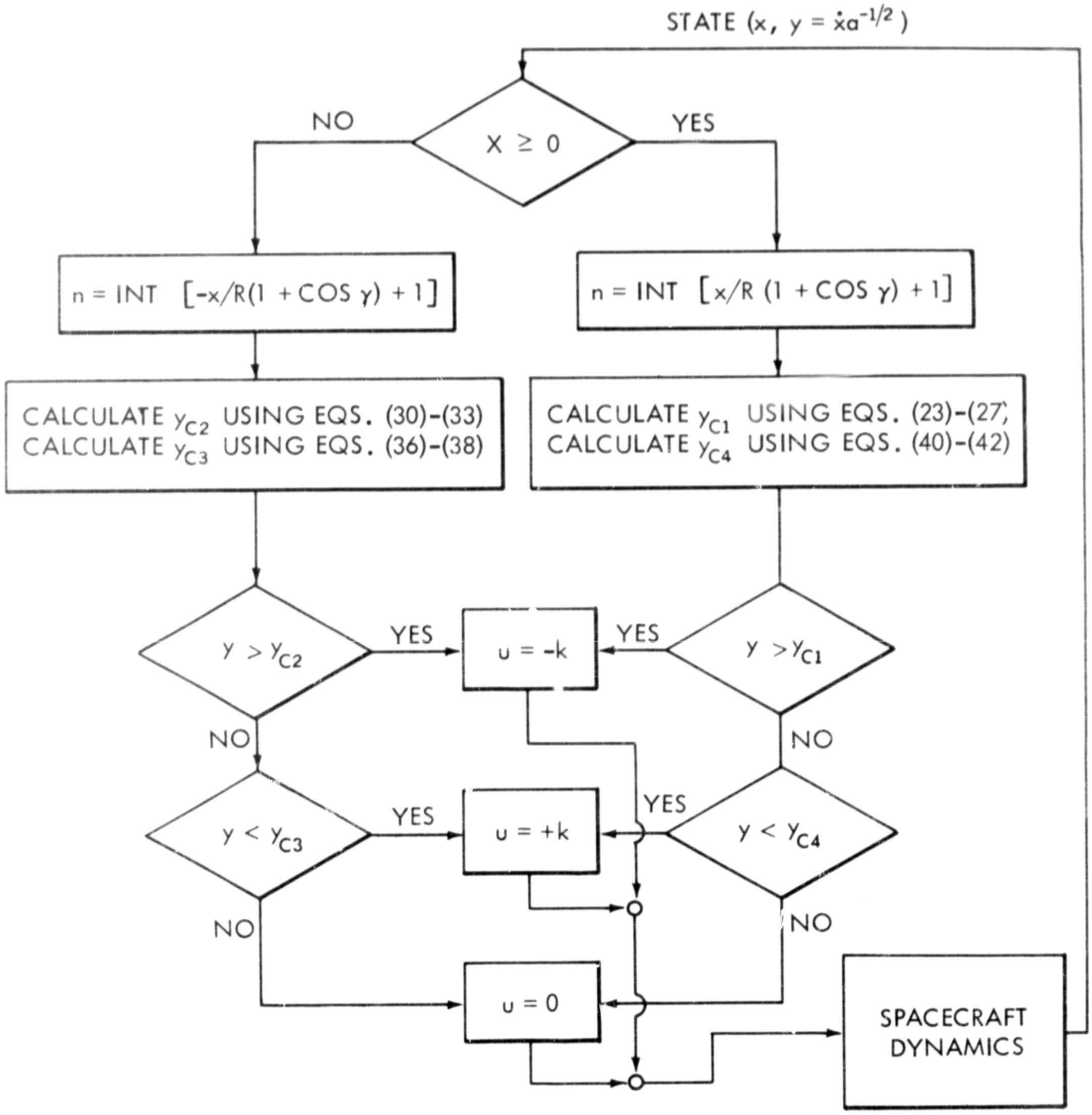

Figure 6. Flowchart for implementation of the time/fuel optimal control law

INT (x) = integer of the number x.

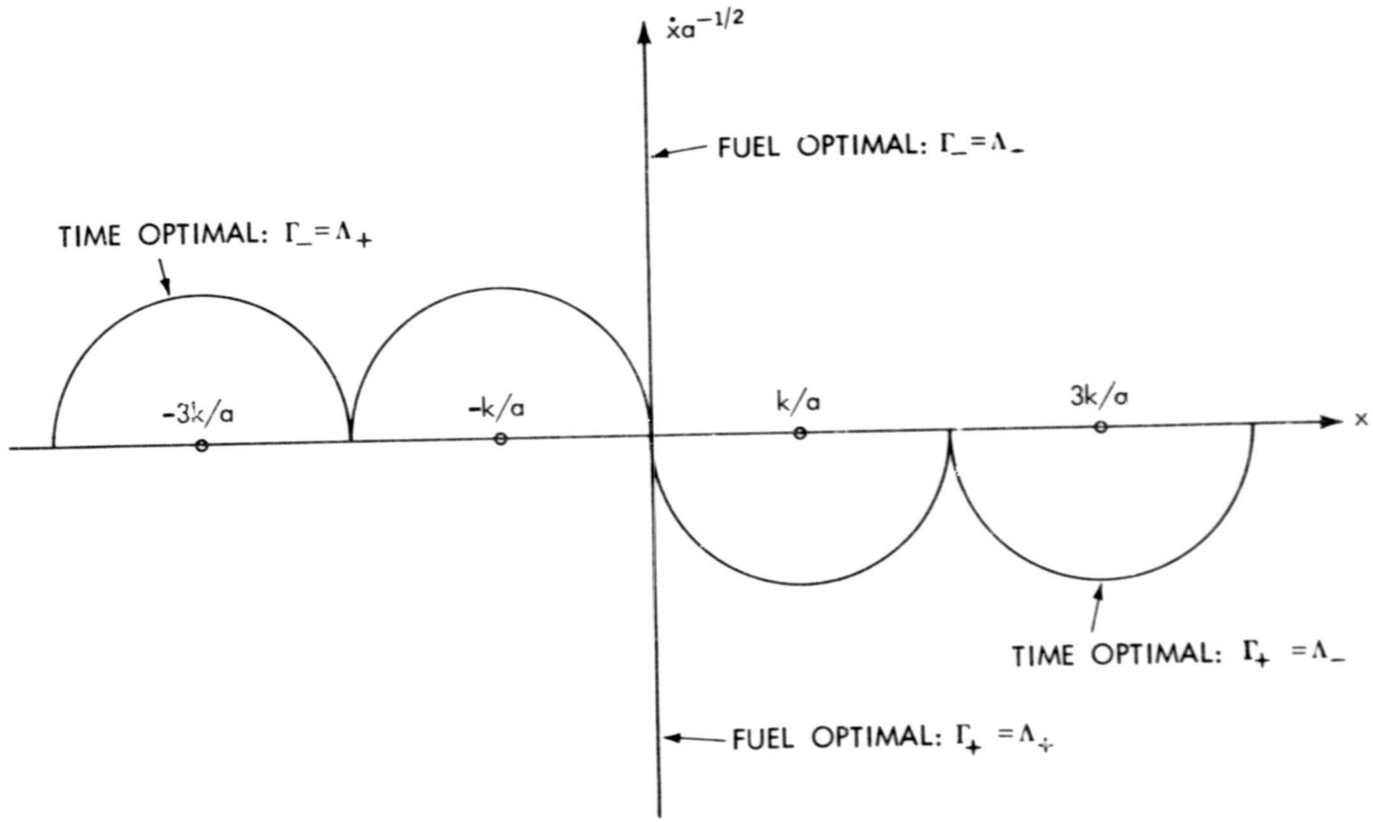

Figure 7. Reduction of the combined time-fuel optimal switching lines to the pure time optimal case ($\gamma = 0°$) and to the pure fuel optimal case ($\gamma = 180°$). The switching line for the latter case falls into the $\dot{x}a^{-1/2}$-axis.